International Journal of Computer Information Systems and Industrial Management Applications
ISSN 2150-7988 Volume 18(18s) 2026 pp. 45-64
https://doi.org/10.70917/ijcisim-2026-4836
Article

Therapeutic potential of Psidium guajava leaf phytochemicals against hepatic encephalopathy: A target-specific drug discovery approach

Debasis Patra[1], Biswa Mohan Sahoo[1], Kakun Das[1], Shilpi Mondal[1], Ashirbad Nanda[1],*

[1]School of Pharmacy and Life Sciences, Centurion University of Technology and Management, Odisha, India
*Corresponding author ashirbadnanda@gmail.com (AN)

Abstract: Psidium guajava L., leaves have long been valued in traditional medicine, including hepatoprotective effects with a rich phytochemical composition responsible for diverse. However, their target-specific therapeutic potential against hepatic encephalopathy (HE) remains underexplored. HE is a serious neuropsychiatric disorder resulting from the accumulation of neurotoxins, particularly ammonia, due to impaired liver detoxification. In this study, we adopted an integrative computational approach to explore the therapeutic efficacy of P. guajava leaf-derived phytochemicals against three key HE-related protein targets identified via the GeneCards database: sodium channel protein type 1 subunit alpha/SCN1A (PDB ID: 6AGF), glycine decarboxylase/GLDC (PDB ID: 6I33), and potassium voltage-gated channel subfamily Q member 2/KCNQ2 (PDB ID: 8X43). A total of 89 phytochemicals, along with three standard drugs' binding efficacy were validated through molecular docking using PyRx 0.8-AutoDock 4.2 software, where several phytocompounds demonstrated stronger binding affinities than standard drugs. Further physicochemical, toxicity, pharmacokinetic, and drug-likeness studies were predicted, where PG_LP21 (guaijaverin) and PG_LP75 (rutin) were selected as two lead compounds with favorable drug-likeness profiles. Further, the lead compounds (PG_LP75/rutin) along with their standard drug (SD1/carbamazepine) stability and reactivity were investigated through molecular dynamics (MD) simulations at 100 nanoseconds, and free energy calculation (MM/PBSA) along with HOMO–LUMO analysis supported that PG_LP75 has higher stability. Overall, this study highlights a novel target-specific computational strategy linking traditional herbal knowledge with modern drug discovery, offering promising leads for HE therapeutics from P. guajava.
Keywords: Psidium guajava leaves, Hepatic encephalopathy, Molecular docking-dynamics simulation, Toxicity and drug-ability assessment

1. Introduction

Hepatic encephalopathy (HE) is a major neuropsychiatric complication associated with liver dysfunction (1-3). Based on physiological condition, it has categories such as cognitive impairment, confusion, altered levels of consciousness, and, in severe cases, coma (1-3). Primarily, it arises through the accumulation of neurotoxins such as ammonia, which the compromised liver adequately fails to detoxify, wherein acute or chronic forms are commonly associated with advanced liver diseases such as cirrhosis, hepatitis, and portal hypertension (2, 5, 6). Globally, the prevalence of HE among cirrhotic patients ranges from 30% to 45%, while covert HE affects approximately 60% to 80% of this population (7-9). According to recent epidemiological reports, nearly 1 to 2 million deaths globally are recorded per annum, mostly arising from liver cirrhosis (10, 11). Late diagnosis, limited access to specialized care, and high treatment costs exacerbate the burden in India and other low-to-middle-income countries (4, 8, 10). As per the reports. 10%–50% of hospitalized patients with cirrhosis also have HE, and the death rates for these patients while in the hospital range from 15% to 40% in the Indian scenario (12-14).

Advancements in medical diagnosis have explored the pathophysiology of HE (1,2). However, current therapeutics are limited to lactulose, rifaximin, and branched-chain amino acids, which provide moderate efficacy but also come with adverse effects and poor patient compliance (15-19). Newer potent and non-toxic therapy is needed

for the management of HE. As a result, complementary and alternative medicine (CAM), mainly herbal and nutraceutical-based interventions, is well-known to be safer and cost-effective, along with having the multimodal ability to counter HE (20, 21). Nonetheless, natural remedies have been explored for HE management, including the most hepatoprotective and antioxidant herbal regimes: silymarin from *Silybum marianum*, andrographolide from *Andrographis paniculata*, and curcumin from *Curcuma longa* modulating oxidative stress and inflammatory pathways involved in hepatic and neural dysfunction (22-25). In addition, herbal extracts of *Phyllanthus niruri, Boerhavia diffusa, Tinospora cordifolia*, and *Glycyrrhiza glabra* have also been studied for their hepatorestorative properties in preclinical models of hepatic toxicity and encephalopathy and showed effectiveness, but it was limited to the crude form as a traditional approach, which is not suitable for modern drug discovery (26-28).

With a growing repository of herbal interventions for HE, *Psidium guajava* L., (guava) leaves stand out due to their long-standing use in traditional medicine (29-32). Traditionally, guava leaves have been consumed for treating liver ailments, digestive disorders, and febrile conditions. Along with that, guava leaf teas have been used to alleviate symptoms of early-stage hepatic dysfunction and mental fatigue, both characteristic of minimal symptoms of HE. As per the traditional claim record, it has recorded hepatoprotective, antioxidant, anti-inflammatory, antidiarrheal, antimicrobial, and neuroprotective properties (31, 33). Importantly, guava leaves are rich in bioactive phytochemicals such as quercetin, catechin, rutin, gallic acid, ferulic acid, ellagic acid, etc., which are known to modulate oxidative stress, neuronal signalling, and inflammatory cascades, key contributors to the development and progression of HE (29-31). Given their favorable safety profile as nutritional fruits, guava leaf phytochemicals represent a promising alternative for drug discovery, and several parallel research projects are going on.

A target-specific scientific exploration of *P. guajava* leaf constituents against HE-related molecular pathways is warranted to validate and harness these traditional claims for modern therapeutic applications (34-36). The present systematic and rational strategy to identify bioactive and drug-lead phytochemicals for managing HE. With traditional support of non-specific neuroprotective properties, we have investigated the efficacy against HE pathogenesis-associated putative target protein from the GeneCards database. To bridge traditional herbal knowledge with molecular pharmacology relevance, the present study addresses this critical gap by adopting an integrative *in silico* approach to assess the therapeutic potential of guava leaf-derived phytochemicals against HE. To the best of our knowledge, this paper is the first comprehensive target-specific computational evaluation of *P. guajava* phytochemicals in the context of HE. This multi-level computational framework provides a rational and cost-effective strategy for identifying promising leads for future drug development against HE with higher experimental and clinical success (36, 37).

2. Materials and Methods

2.1. Selection and retrieval of phytochemicals reported from P. guajava leaves

An extensive literature review gathered a comprehensive list of phytochemicals from *P. guajava* leaves, where a total of 89 (PG_LP1 to PG_LP89) belonging to different phytochemical classes were selected (Table S1). The literature search was conducted independently across PubMed, Scopus, Google Scholar, ScienceDirect, Wiley, and Springer databases using the keyword combinations '*Psidium guajava*' or 'guava' and ('leaf' or 'leaves') and ('phytochemical' or 'chemical constituent' or 'secondary metabolite' or 'phytoconstituent,' without any date and year restriction. Original research articles, phytochemical/GC-MS profiling studies, and review articles on phytochemicals reported from *P. guajava* leaves (any solvent extract) were included. Exclusively from other plant parts (fruit, bark, seed, and root) or from other Psidium species, 89 phytochemicals without any duplication (PG_LP1-PG_LP89) were selected for the present study. Further chemical structures were retrieved from the PubChem database; where those were not available in PubChem, chemical structures were manually drawn using ChemDraw 20.0 software. The Simplified Molecular Input Line-Entry System (SMILES) notations were generated to use in various cheminformatics and bioinformatics predictions (36, 38). Before the docking study, structural optimizations were performed using Avogadro 1.95 software with the Merck Molecular Force Field 94s (MMFF94s), and all optimized structures were subsequently saved in PDB format (36, 38).

2.2. Target protein selection, and retrieval for molecular docking study

To use the most putative target along with literature, we have used the GeneCard database record and selected three target proteins associated with HE pathophysiology. Simply perform a search in the GeneCards database (www.genecards.org, version 5.20) for the keyword 'hepatic encephalopathy' and obtain a list of genes associated with HE, further sorted by the GeneCards relevance score in descending order and filtered to retain only 'protein coding' gene category entries. Based on this ranking, the top ten protein-coding genes by relevance score were selected, and three targets (GLDC, SCN1A, and KCNQ2) were finally selected based on (i) their rank in relevance score within this top ten; (ii) documented mechanistic association with ammonia/glycine metabolism and neuronal hyperexcitability relevant to HE pathophysiology in the literature; and (iii) the availability of an experimentally resolved, ligand-amenable 3D structure in the RCSB Protein Data Bank (Fig. S1; 39-41). For the molecular docking study, the 3D protein structures were retrieved from the Protein Data Bank: SCN1A (PDB ID: 6AGF), GLDC (PDB ID: 6I33), and KCNQ2 (PDB ID: 8X43), and all heteroatoms, water molecules, and additional chains were removed, along with remodelling the structure to make up the missing residual (38, 43). To compare the therapeutic potency, three standard drugs (SDs) for each target were used: carbamazepine (SCN1A), pyridoxal phosphate (GLDC), and ezogabine (KCNQ2), respectively. Docking studies were conducted using the PyRx 0.8-AutoDock 4.2 software with user-defined grid boxes created around the active sites of each target protein, and ten different binding poses were generated for each compound against each target (38, 43). The lowest binding energy conformation (kcal/mol.) was selected as the optimal pose, and protein-ligand interaction was performed using BIOVIA Discovery Studio Visualizer 2019 (BIOVIA-DSV-2019) to examine the hydrogen bonding, hydrophobic interactions, van der Waals forces, pi–pi stacking, and electrostatic interactions (38, 43).

2.3. Physicochemical, toxicity, and pharmacokinetics profile prediction

We have predicted the oral drug-likeness and pharmacokinetic properties of phytochemicals using various bioinformatics web tools. All 89 phytochemicals and three standard drugs were submitted as canonical SMILES to SwissADME (http://www.swissadme.ch) and ProTox 3.0 (https://tox.charite.de/protox3) were used for predictions, and each compound was processed individually. The physicochemical properties, referred to as Lipinski's Rule of Five (Ro5), included parameters such as molecular weight, lipophilicity (XlogP), hydrogen bond donors (HBD), hydrogen bond acceptors (HBA), and topological polar surface area (tPSA), which were recorded from the SwissADME tool (42, 43). Various toxicity profiles, including hepatotoxicity (HT), neurotoxicity (NueT), nephrotoxicity (NepT), cardiotoxicity (CrT), carcinogenicity (CG), immunotoxicity (IT), mutagenicity (MG), and cytotoxicity (CT), along with respiratory toxicity (RT) and ecotoxicity (ET), as well as overall toxicity class (TC) and median lethal dose (LD_{50}, mg/kg), were predicted using the ProTox 3.0 tool (42, 43). Toxicity endpoints were reported by ProTox 3.0 as a binary active/inactive prediction with an associated confidence probability (0–1) generated from its default machine-learning classification models; TC (toxicity class) followed the GHS-based scheme used by the tool (Class I–III, LD50 ≤5 to ≤300 mg/kg, more hazardous; Class IV–VI, LD50 >300 to ≤5000 mg/kg, less hazardous). Pharmacokinetic profiling, such as gastrointestinal (GI) absorption, blood–brain barrier (BBB) permeability, P-glycoprotein (P-gp) substrate prediction, and bioavailability (BA) score, was also recorded from SwissADME to understand the systemic behaviour of phytochemicals (42, 43).

2.4. Drug-likeness score prediction and frontier molecular orbital analyses

To select the most potential lead, drug-likeness (DL) scores of each phytochemical were predicted using the Molsoft tool (www.molsoft.com/mprop; 42, 43). All structures were submitted as canonical SMILES to the Molsoft server, using default settings. Further, to understand the relationship between chemical structure and biological activity, Structure–Activity Relationship (SAR) analysis was carried out within lead phytochemicals. Further, the

chemical reactivity and stability of the lead compounds were observed based on the Highest Occupied Molecular Orbital (HOMO) and Lowest Unoccupied Molecular Orbital (LUMO) surface energies and their energy gap (ΔEH–L). Using the single-point energy calculations approach with the Restricted Hartree–Fock (RHF) method prior geometry optimization to a convergence gradient of 10^{-4} Hartree/Bohr, the analyses were carried out using Avogadro 1.2.0 integrated with the ORCA 5.0 quantum chemistry package (42, 43).

2.5. Molecular dynamics simulation and free-energy calculation

The dynamic behaviour and stability of the lead protein-ligand docking complex (SCN1A-PG_LP75/Rutin) along with the standard drug (SCN1A-SD_1/carbamazepine) were simulated using MD simulations performed at 100 nanoseconds. Note that based on docking scores, toxicity, and DL-scores, PG_LP75/Rutin was selected as the lead phytochemical for MD simulations. SCN1A was prioritized for MD/MM-PBSA analysis over GLDC and KCNQ2 because it returned the highest and most consistent docking scores across the top-ranked phytochemical set (Table 1) and because a well-characterized standard drug (carbamazepine) was available for direct benchmarking; extending MD validation to the GLDC and KCNQ2 complexes was beyond the computational scope of the present study and is identified as a priority for follow-up work (see Discussion). All-atom MD simulations were carried out using GROMACS 2020.4 software, applying the AMBER99SB-ILDN force field (42, 43). Each protein-ligand complex was centred in a cubic simulation box with a minimum solute-to-boundary distance of 1.0 nm and periodic boundary conditions applied in all three dimensions.

The ACPYPE server calculated the parameters and topologies of the ligands (using the General Amber Force Field, GAFF, with AM1-BCC partial atomic charges) before going to MD simulations of complexes using the TIP3P water-filled model (42, 43). Further, the system neutralization was achieved by adding 50 Na+ ions (and an equal number of Cl- counter-ions where required) to achieve overall charge neutrality at a physiological ionic strength of 0.15 M NaCl, followed by the energy minimization step, which was performed using the 50,000 steepest descent method using a Fourier grid, and estimated the relative computational load with a load of the Particle Mesh Ewald (PME) 1.2 nm (42, 43). Energy minimization was continued until the maximum force on any atom fell below 1000 kJ/mol/nm (Fmax <1000 kJ/mol/nm), confirming that the system had reached a locally relaxed, artefact-free starting configuration. After the energy minimization step, the NVT and NPT equilibrations were performed to equilibrate the system for a 100 ps time scale for each (42, 43). Temperature was maintained at 300 K using the V-rescale (modified Berendsen) thermostat, and pressure was maintained at 1 bar using the Parrinello-Rahman barostat during NPT equilibration; a 2 fs integration time step was used throughout, with all bonds involving hydrogen constrained using the LINCS algorithm, and the production MD run (100 ns) trajectory frames were saved every 10 ps for subsequent analysis. After completing the final MD step, further MD trajectories were used for calculating the RMSD (root mean square deviation) and RMSF (root mean square fluctuation), radius of gyration (Rg), and hydrogen-bond plots were generated using the Xmgrace tool (42, 43). In addition, the MM/PBSA (Molecular Mechanics/Poisson-Boltzmann Surface Area) method was used to calculate the free energy (ΔGbind) of both docking complexes using the g_mmpbsav5.12 suites (42, 43). Based on molecular mechanic energy, the total free energy along with common residues in both complexes was observed.

3. Results

3.1. Molecular docking study

The docking score (kcal/mol.) of phytochemicals along with the SDs was recorded in Table 1. The docking score revealed that phytochemicals showed docking scores within -5 to -12 kcal against SCN1A, -4 to -10 against GLDC, and -4 to -9 against KCNQ2. In addition, phytochemicals such as PG_LP78 (-11.1), PG_LP79 (-11.0), PG_LP63 (-10.8), PG_LP26 (-10.5), PG_LP27, PG_LP37, PG_LP88 (-10.2), PG_LP43, PG_LP50, and PG_LP75 (-10.1) are some potential candidates against SCN1A. Similarly, PG_LP60 (-9.4), PG_LP63, PG_LP64, PG_LP74, PG_LP74 (-9.0), PG_LP37, PG_LP54, PG_LP59, PG_LP75 (-8.9), PG_LP56, and PG_LP57 (-8.7); PG_LP26 (-8.5), PG_LP81 (-8.4), PG_LP27 (-8.3), PG_LP30 (-8.2), PG_LP57 (-8.1), PG_LP43, PG_LP56, PG_LP61, and PG_LP72

(-8.0) against KCNQ2 (Table 1). Overall, some phytochemicals showed stronger binding efficacy than standard drugs, especially against SCN1A among three targets. As per the distinct binding affinity of phytochemicals against three targets, we have calculated the average docking score where PG_LP63 (-9.06), PG_LP75 (-8.93), PG_LP37 (-8.90), PG_LP57 and PG_LP79 (-8.86), and PG_LP43, PG_LP56, and PG_LP81 (-8.73) selected some potential lead phytochemicals. Again, towards more clarity, we have selected the top 25 lead candidates from each target, including average docking, and found out the common candidates through a Venn diagram (Fig. 1). Based on the Venn diagram, we found that seven phytochemicals, PG_LP37, PG_LP75, PG_LP57, PG_LP56, PG_LP81, PG_LP22, and PG_LP21, are considered as lead candidates (Fig. 1). As representative protein-ligand interactions, we have elucidated the SCN1A-PG_LP75/Rutin along with their standard drug docking complex (SCN1A-SD_1/Carbamazepine) interactions in both 3D and 2D images (Fig. 2), where, compared to the standard drug, PG_LP75 showed more H-bond interactions with pi-pi and pi-alkyl interactions, which supported the higher docking score and stronger binding efficacy than standard drugs (Fig. 2).

Table 1: Molecular docking score and drug-ability of phytochemicals and standard drugs.

Code used	**Docking score**	**Docking score**	**Docking score**	**Docking score**	**Drug-ability profiles**	**Drug-ability profiles**	**Drug-ability profiles**	**Drug-ability profiles**	**Drug-ability profiles**	**Drug-ability profiles**
Code used	SCN1A	GLDC	KCNQ2	Avg.	Ro5	WS	BA	SA	DL	LD50
PG_LP1	-8.7	-8.1	-7.1	-7.96	Yes	S	0.55	2.96	0.39	2500
PG_LP2	-8.7	-7.6	-7.4	-7.90	Yes	PS	0.56	0.56	0.77	2000
PG_LP3	-8.8	-8.4	-7.8	-8.33	No	S	0.17	2.04	0.60	5000
PG_LP4	-9.5	-8.3	-7.1	-8.30	Yes	PS	0.55	5.68	-0.13	2000
PG_LP5	-9.3	-8.4	-7.4	-8.36	Yes	PS	0.85	5.63	0.25	2610
PG_LP6	-8.5	-6.0	-6.8	-7.10	No	S	0.55	4.51	-1.74	5300
PG_LP7	-7.5	-6.3	-5.6	-6.46	Yes	S	0.55	3.95	0.07	2830
PG_LP8	-6.4	-6.3	-5.7	-6.13	Yes	VS	0.55	1.31	-0.35	2980
PG_LP9	-7.3	-7.0	-6.4	-6.90	Yes	S	0.55	4.35	-1.50	5000
PG_LP10	-8.0	-7.9	-7.1	-7.66	Yes	S	0.55	3.50	0.64	10000
PG_LP11	-8.0	-8.5	-7.1	-7.86	No	VS	0.11	4.16	0.79	5000
PG_LP12	-6.2	-6.3	-5.6	-6.03	Yes	S	0.85	1.67	-1.17	2500
PG_LP13	-9.6	-8.3	-7.3	-8.40	No	PS	0.56	6.34	0.60	2000
PG_LP14	-8.8	-7.8	-7.6	-8.06	Yes	S	0.55	3.17	-1.11	2991
PG_LP15	-7.8	-7.5	-7.0	-7.43	Yes	S	0.55	3.50	0.64	10000
PG_LP16	-8.4	-8.4	-7.6	-8.13	No	S	0.17	4.20	0.23	1000

PG_LP17	-6.0	-5.3	-5.1	-5.46	Yes	S	0.55	3.65	-1.04	2480
PG_LP18	-6.5	-7.5	-5.8	-6.60	Yes	S	0.85	1.93	-0.61	1772
PG_LP19	-6.3	-6.2	-5.4	-5.96	Yes	VS	0.56	1.22	-0.22	2000
PG_LP20	-9.0	-5.8	-7.6	-7.46	Yes	PS	0.55	4.91	-0.78	1140
PG_LP21	-9.8	-8.5	-7.7	-8.66	No	S	0.17	5.05	0.93	5000
PG_LP22	-9.2	-8.3	-7.8	-8.43	Yes	PS	0.55	5.71	-0.50	1140
PG_LP23	-8.3	-8.5	-7.3	-8.03	Yes	MS	0.55	4.73	-0.70	1140
PG_LP24	-9.3	-7.9	-7.3	-8.16	No	PS	0.56	6.52	0.40	5000
PG_LP25	-7.5	-8.0	-6.3	-7.26	No	MS	0.17	5.25	0.79	12000
PG_LP26	-10.5	-7.3	-8.5	-8.76	No	MS	0.17	5.58	0.80	2190
PG_LP27	-10.2	-7.0	-8.3	-8.50	No	MS	0.17	5.61	0.85	5000
PG_LP28	-8.3	-8.3	-7.4	-8.00	Yes	S	0.55	4.89	0.68	2000
PG_LP29	-7.7	-8.1	-7.4	-7.73	Yes	S	0.55	5.00	0.01	2000
PG_LP30	-7.9	-7.6	-8.2	-7.90	No	VS	0.11	4.93	0.72	2260
PG_LP31	-8.3	-7.9	-7.6	-7.93	No	S	0.17	5.32	0.68	5000
PG_LP32	-8.3	-6.5	-6.4	-7.06	Yes	S	0.55	4.51	-1.74	5300
PG_LP33	-7.9	-8.0	-7.2	-7.70	No	S	0.17	5.32	0.68	5000
PG_LP34	-8.0	-7.7	-7.0	-7.56	Yes	S	0.55	3.14	0.50	3919
PG_LP35	-6.3	-5.9	-5.2	-5.80	Yes	S	0.55	3.48	-1.54	4400
PG_LP36	-5.3	-5.4	-4.7	-5.13	Yes	S	0.55	2.74	-0.99	2200
PG_LP37	-10.2	-8.9	-7.6	-8.90	Yes	PS	0.55	5.49	-0.22	2000

PG_LP38	-8.0	-8.0	-7.5	-7.83	Yes	S	0.55	3.02	0.38	3919
PG_LP39	-10.0	-8.3	-7.3	-8.53	Yes	PS	0.56	6.22	0.55	2000
PG_LP40	-6.5	-5.8	-5.3	-5.86	Yes	VS	0.55	1.50	-0.65	1700
PG_LP41	-8.3	-7.7	-7.4	-7.80	Yes	S	0.55	3.25	0.46	3919
PG_LP42	-8.5	-7.8	-7.3	-7.86	Yes	S	0.55	3.27	-0.24	159
PG_LP43	-10.1	-8.1	-8.0	-8.73	Yes	PS	0.85	6.08	0.37	2000
PG_LP44	-6.1	-6.0	-5.4	-5.83	Yes	VS	0.56	1.07	0.23	2000
PG_LP45	-9.0	-7.6	-7.7	-8.10	Yes	PS	0.55	5.71	-0.50	1140
PG_LP46	-7.8	-7.4	-7.5	-7.56	Yes	PS	0.55	5.08	-0.12	1140
PG_LP47	-5.1	-4.6	-4.1	-4.60	Yes	PS	0.55	5.21	-0.15	690
PG_LP48	NP	NP	NP	NP	Yes	PS	0.55	5.50	0.08	1140
PG_LP49	-5.2	-4.7	-4.1	-4.66	Yes	PS	0.55	5.50	0.08	1140
PG_LP50	-10.1	-7.8	-6.6	-8.16	Yes	PS	0.55	5.71	0.84	1140
PG_LP51	-5.1	-4.7	-4.1	-4.63	Yes	PS	0.55	5.71	0.84	1140
PG_LP52	NP	NP	NP	NP	Yes	PS	0.55	5.08	-0.12	1140
PG_LP53	NP	NP	NP	NP	Yes	PS	0.55	4.97	0.38	1140
PG_LP54	-9.3	-8.9	-7.4	-8.53	Yes	S	0.55	1.80	-1.15	1840
PG_LP55	-9.8	-8.0	-7.0	-8.26	No	PS	0.56	6.55	0.85	5000
PG_LP56	-9.5	-8.7	-8.0	-8.73	Yes	MS	0.55	3.66	0.16	2000
PG_LP57	-9.8	-8.7	-8.1	-8.86	Yes	MS	0.55	3.66	0.16	2000
PG_LP58	-8.1	-7.8	-7.9	-7.93	Yes	PS	0.55	5.97	-0.51	2148

PG_LP59	-8.9	-8.9	-7.8	-8.53	Yes	PS	0.55	5.90	-0.30	1140
PG_LP60	-8.3	-9.4	-7.2	-8.30	Yes	PS	0.55	5.67	-0.29	500
PG_LP61	-8.9	-7.4	-8.0	-8.10	Yes	PS	0.55	5.62	-0.56	1140
PG_LP62	-8.4	-7.9	-7.8	-8.03	Yes	PS	0.55	5.62	-0.56	1140
PG_LP63	-10.8	-9.0	-7.4	-9.06	Yes	PS	0.56	6.45	0.41	2000
PG_LP64	-7.9	-9.0	-7.1	-8.00	Yes	PS	0.55	5.90	-0.30	1140
PG_LP65	-8.5	-7.9	-7.1	-7.83	Yes	PS	0.55	5.90	-0.30	1140
PG_LP66	-8.4	-7.8	-7.4	-7.86	Yes	PS	0.55	5.90	-0.30	1140
PG_LP67	-7.1	-7.2	-6.4	-6.90	Yes	S	0.55	3.67	-0.27	1800
PG_LP68	-6.2	-4.5	-4.9	-5.20	Yes	PS	0.55	4.91	0.99	6800
PG_LP69	-9.1	-8.5	-7.4	-8.33	No	MS	0.17	7.94	0.72	4000
PG_LP70	-8.1	-7.8	-7.2	-7.70	Yes	S	0.55	3.23	0.52	159
PG_LP71	-8.7	-8.0	-7.8	-8.16	Yes	S	0.11	3.45	0.37	5000
PG_LP72	-8.5	-8.0	-8.0	-8.16	No	S	0.17	5.32	0.68	5000
PG_LP73	-8.5	-8.1	-7.2	-7.93	No	S	0.17	5.05	0.93	5000
PG_LP74	-8.8	-9.0	-7.5	-8.43	No	S	0.17	5.05	0.93	5000
PG_LP75	-10.1	-8.9	-7.8	-8.93	No	S	0.17	6.52	0.91	5000
PG_LP76	-8.3	-8.6	-4.6	-7.16	Yes	VS	0.56	1.70	-0.81	1700
PG_LP77	-6.4	-6.2	-5.3	-5.96	Yes	VS	0.56	1.70	-0.81	1700
PG_LP78	-11.1	-5.7	-7.4	-8.06	Yes	PS	0.85	6.21	0.66	2000
PG_LP79	-11.0	-8.4	-7.2	-8.86	Yes	PS	0.55	6.28	0.20	4300

PG_LP80	-6.1	-5.7	-5.1	-5.63	Yes	S	0.85	1.42	-0.18	2000
PG_LP81	-9.3	-8.5	-8.4	-8.73	Yes	PS	0.56	6.34	0.60	2000
PG_LP82	-8.0	-5.8	-6.8	-6.86	Yes	MS	0.55	5.53	-1.63	5000
PG_LP83	-7.8	-6.2	-6.6	-6.86	Yes	S	0.55	4.67	-0.89	3700
PG_LP84	-8.0	-6.3	-6.7	-7.00	Yes	S	0.55	3.66	-1.42	3650
PG_LP85	-6.2	-4.9	-5.2	-5.43	Yes	S	0.55	4.44	-1.45	3700
PG_LP86	-6.4	-6.2	-5.1	-5.90	Yes	S	0.55	3.24	-1.05	2830
PG_LP87	-7.6	-6.5	-6.6	-6.90	Yes	S	0.55	3.38	-0.60	2000
PG_LP88	-10.2	-8.0	-7.4	-8.53	Yes	PS	0.55	6.30	0.78	890
PG_LP89	-7.9	-6.6	-6.7	-7.06	Yes	S	0.55	4.35	-1.09	4400
SD_1*	-9.2	-----	----	-9.2	Yes	S	0.55	4.35	0.67	5010
SD_2*	----	-6.3	----	-6.3	No	PS	0.17	4.47	1.03	1000
SD_3*	----	----	-6.7	-6.7	Yes	PS	0.53	6.61	0.39	500

WA, water-soluble; MS, moderately soluble; PS, poorly soluble; S, soluble; VS, very soluble; SA, synthetic accessibility; DL, drug-likeness; BA, bioavailability; NP, not applicable.

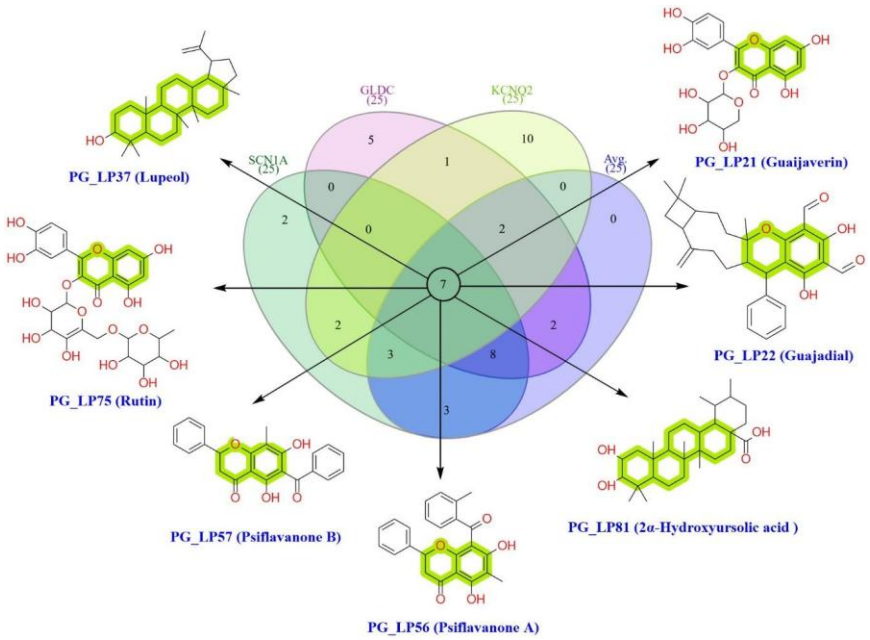

Figure 1: Based on individual and average docking scores, we have selected seven potential phytochemicals against three putative target proteins associated with hepatic encephalopathy. The potent phytochemicals are presented in a Venn diagram, along with their chemical structure (core moiety highlighted in a green color) using ChemDraw 2020 software.

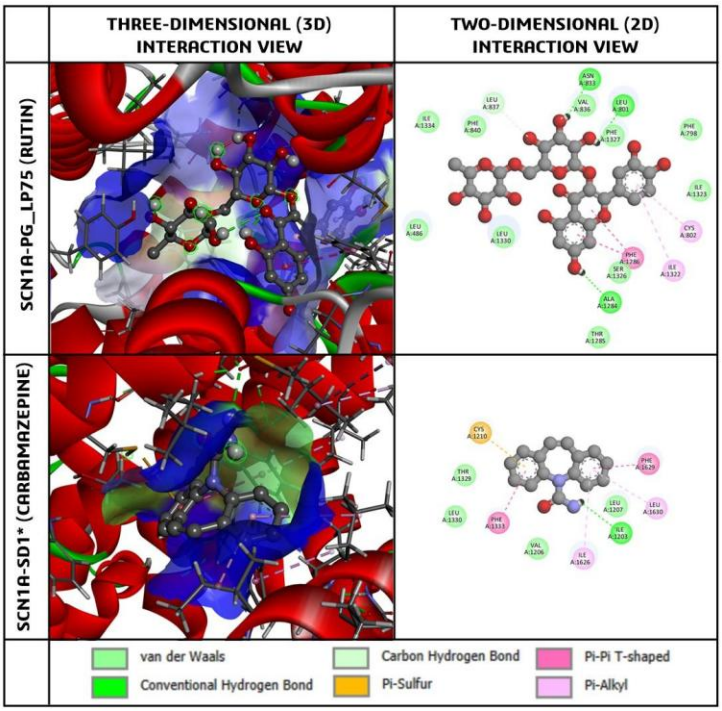

Figure 2: Protein-ligand interaction of one of the lead phytochemicals, PG_LP75 (rutin), and a reference standard drug, SD1 (carbamazepine), against the putative target protein, sodium voltage-gated channel alpha subunit 1 (SCN1A), in 3D and 2D interactive views. The images were generated through BIOVIA Discovery Studio Visualizer and presented overall using ChemDraw 2020 software.

3.2. Physicochemical, toxicity, and pharmacokinetics profile prediction

The physiological, or Ro5, profiles of all phytochemicals along with standard drugs were predicted, and we have found that among 89 phytochemicals, only 19 phytochemicals, including the lead (PG_LP75 and PG_LP21) and SD_2, do not follow the Ro5 due to higher molecular weight (> 500 g/mol.). Existing drugs, vincristine, taxol, rifampicin, vancomycin, etc., are still used as mainstream drugs without obeying the Ro5 rules. Therefore, Ro5 is guided towards orally active candidates, but strict implementation may have eliminated a number of bioactive candidates at an early stage. As per the records, distinct toxicity profiles of phytochemicals were recorded, where a moderate to higher risk of nephrotoxicity (NepT), respiratory toxicity (RT), and a higher risk of immunotoxicity (IT) than the rest of the toxicity profiles are safe, as indicated in green color (Table 2). Similarly, standard drugs also showed a higher risk of NeuT, NepT, and IT and a moderate toxicity of HT and carcinogenicity (Table 2). The two lead phytochemicals, PG_LP21 and PG_LP75, also showed a high risk of NepT and IT. From toxicity class (TC), except PG_LP42 and PG_LP70, most phytochemicals and standard drugs are safe at higher concentrations (300 mg/kg < LD50 > 5000 mg/kg) as they fall in the class IV to VI category. After potency, toxicity profiles are also in favor of phytochemicals to be used as potential and safer candidates for the management of HE. Based on the BA and WS profiles, the distinct pharmacokinetic profiles were also recorded (Table S2). A few phytochemicals, such as PG_LP7, PG_LP9, PG_LP12, PG_LP17, PG_LP18, PG_LP35, PG_LP54, PG_LP67, PG_LP83, PG_LP85, PG_LP86, and PG_LP87, showed BBB permeability profiles, indicating those could be favorable for neuroprotective therapeutic agents, but HE is a complex disease associated with and regulated by different pathways, and there is no need to

directly target the brain (Table S2). Overall, each phytochemical did not obey all ideal drug parameters but overall showed that among seven lead phytochemicals, PG_LP21 and PG_LP75 are two ideal candidates. Note that all parameters are predicted based on training set datasets, and they may vary in living systems. In addition, the prediction profiles help with the early assessment of drug-ability profiles and suggest implementing platforms like structural modification or nano-formulation to optimize the profiles to improve the solubility and pharmacokinetics for better therapeutic outcomes ().

Table 2: Predicted toxicity profiles of phytochemicals and standard drugs.

Code	HT	NeuT	NepT	CD	CT	IT	MT	CT	TC
PG_LP1	IA(0.68)	IA(0.86)	A(0.60)	IA(0.63)	IA(0.62)	IA(0.99)	IA(0.57)	IA(0.87)	V
PG_LP2	IA(0.91)	IA(0.93)	IA(0.51)	A(0.57)	IA(0.70)	A(0.77)	IA(0.81)	IA(0.73)	IV
PG_LP3	IA(0.80)	IA(0.88)	A(0.72)	IA(0.61)	IA(0.79)	A(0.68)	IA(0.73)	IA(0.72)	V
PG_LP4	IA(0.88)	IA(0.66)	IA(0.82)	A(0.79)	IA(0.65)	IA(0.50)	IA(0.79)	IA(0.98)	IV
PG_LP5	IA(0.54)	IA(0.79)	IA(0.60)	A(0.67)	A(0.53)	A(0.74)	IA(0.71)	IA(0.97)	V
PG_LP6	IA(0.80)	IA(0.51)	IA(0.92)	IA(0.81)	IA(0.70)	IA(0.54)	IA(0.95)	IA(0.75)	V
PG_LP7	IA(0.78)	IA(0.62)	IA(0.87)	IA(0.77)	IA(0.70)	IA(0.97)	IA(0.83)	IA(0.75)	V
PG_LP8	IA(0.57)	IA(0.83)	A(0.59)	IA(0.97)	A(0.78)	IA(0.50)	IA(0.98)	IA(0.86)	V
PG_LP9	IA(0.80)	IA(0.57)	IA(0.86)	IA(0.84)	IA(0.57)	A(0.83)	IA(0.88)	IA(0.79)	V
PG_LP10	IA(0.72)	IA(0.90)	A(0.62)	IA(0.99)	IA(0.51)	IA(0.96)	IA(0.55)	IA(0.84)	VI
PG_LP11	IA(0.72)	IA(0.89)	A(0.56)	IA(0.99)	IA(0.68)	A(0.99)	IA(0.93)	IA(0.80)	V
PG_LP12	A(0.54)	IA(0.67)	A(0.55)	IA(0.53)	IA(0.82)	IA(0.95)	IA(0.96)	IA(0.83)	V
PG_LP13	IA(0.65)	IA(0.85)	IA(0.56)	A(0.70)	IA(0.63)	A(0.92)	IA(0.87)	IA(0.89)	IV
PG_LP14	IA(0.83)	IA(0.91)	A(0.58)	IA(0.76)	A(0.59)	IA(0.81)	IA(0.84)	IA(0.90)	IV
PG_LP15	IA(0.72)	IA(0.90)	A(0.62)	IA(0.99)	IA(0.51)	IA(0.96)	IA(0.55)	IA(0.84)	VI
PG_LP16	IA(0.70)	IA(0.88)	A(0.73)	IA(0.89)	A(0.54)	IA(0.89)	IA(0.70)	IA(0.82)	IV
PG_LP17	IA(0.86)	IA(0.59)	IA(0.88)	IA(0.93)	IA(0.68)	IA(0.99)	IA(0.96)	IA(0.75)	V
PG_LP18	IA(0.51)	IA(0.74)	A(0.62)	IA(0.85)	IA(0.61)	A(0.91)	IA(0.96)	IA(0.88)	IV
PG_LP19	IA(0.61)	IA(0.88)	A(0.69)	IA(0.89)	A(0.56)	IA(0.99)	IA(0.94)	IA(0.91)	IV
PG_LP20	IA(0.72)	IA(0.83)	IA(0.61)	IA(0.83)	IA(0.61)	A(0.64)	IA(0.67)	IA(0.83)	IV
PG_LP21	IA(0.80)	IA(0.88)	A(0.75)	IA(0.75)	IA(0.79)	A(0.93)	IA(0.79)	IA(0.69)	V

PG_LP22	IA(0.73)	IA(0.72)	IA(0.60)	IA(0.73)	IA(0.55)	A(0.93)	IA(0.73)	IA(0.82)	IV
PG_LP23	IA(0.77)	IA(0.84)	IA(0.61)	IA(0.81)	IA(0.58)	A(0.71)	IA(0.64)	IA(0.72)	IV
PG_LP24	IA(0.78)	IA(0.90)	A(0.51)	A(0.78)	A(0.59)	A(0.98)	IA(0.93)	IA(0.88)	V
PG_LP25	IA(0.82)	IA(0.89)	A(0.77)	IA(0.56)	IA(0.76)	IA(0.86)	IA(0.81)	IA(0.83)	IV
PG_LP26	IA(0.80)	IA(0.89)	A(0.77)	A(0.51)	IA(0.84)	IA(0.68)	IA(0.82)	IA(0.84)	V
PG_LP27	IA(0.79)	IA(0.89)	A(0.71)	IA(0.68)	IA(0.77)	A(0.74)	IA(0.58)	IA(0.67)	V
PG_LP28	IA(0.84)	IA(0.90)	A(0.77)	A(0.66)	IA(0.82)	IA(0.64)	IA(0.78)	IA(0.84)	IV
PG_LP29	IA(0.84)	IA(0.89)	A(0.77)	A(0.59)	IA(0.85)	IA(0.84)	IA(0.80)	IA(0.83)	IV
PG_LP30	IA(0.70)	IA(0.85)	A(0.75)	IA(0.72)	IA(0.78)	IA(0.85)	IA(0.79)	IA(0.81)	V
PG_LP31	IA(0.82)	IA(0.88)	A(0.76)	IA(0.67)	IA(0.85)	A(0.66)	IA(0.76)	IA(0.69)	V
PG_LP32	IA(0.89)	IA(0.51)	IA(0.92)	IA(0.81)	IA(0.70)	A(0.54)	IA(0.95)	IA(0.75)	V
PG_LP33	IA(0.82)	IA(0.88)	A(0.76)	IA(0.67)	IA(0.85)	A(0.66)	IA(0.76)	IA(0.69)	V
PG_LP34	IA(0.68)	IA(0.89)	A(0.62)	IA(0.91)	IA(0.72)	IA(0.96)	IA(0.52)	IA(0.96)	V
PG_LP35	IA(0.76)	A(0.60)	IA(0.88)	A(0.72)	IA(0.65)	IA(0.95)	IA(0.97)	IA(0.82)	V
PG_LP36	IA(0.76)	IA(0.62)	IA(0.87)	IA(0.75)	IA(0.64)	IA(0.99)	IA(0.95)	IA(0.82)	V
PG_LP37	IA(0.91)	A(0.54)	IA(0.93)	IA(0.86)	IA(0.63)	A(0.57)	IA(0.95)	IA(0.97)	IV
PG_LP38	IA(0.69)	IA(0.89)	A(0.62)	IA(0.99)	A(0.68)	IA(0.97)	A(0.51)	IA(0.99)	V
PG_LP39	IA(0.65)	IA(0.85)	IA(0.56)	A(0.70)	A(0.63)	A(0.61)	IA(0.87)	IA(0.89)	IV
PG_LP40	IA(0.62)	IA(0.83)	A(0.69)	IA(0.73)	IA(0.63)	IA(0.98)	IA(0.91)	IA(0.93)	IV
PG_LP41	IA(0.69)	IA(0.89)	A(0.62)	IA(0.91)	IA(0.72)	A(0.52)	IA(0.52)	IA(0.98)	V
PG_LP42	IA(0.69)	IA(0.89)	A(0.62)	IA(0.99)	A(0.68)	IA(0.86)	A(0.51)	IA(0.99)	III

PG_LP43	A(0.52)	IA(0.74)	IA(0.62)	A(0.71)	A(0.57)	A(0.79)	IA(0.85)	IA(0.99)	IV
PG_LP44	IA(0.59)	IA(0.86)	A(0.61)	IA(0.90)	A(0.72)	IA(0.99)	IA(0.97)	IA(0.90)	IV
PG_LP45	IA(0.73)	IA(0.72)	IA(0.60)	IA(0.73)	IA(0.55)	A(0.93)	IA(0.73)	IA(0.82)	IV
PG_LP46	IA(0.71)	IA(0.87)	IA(0.62)	IA(0.59)	IA(0.58)	A(0.51)	IA(0.61)	IA(0.67)	IV
PG_LP47	IA(0.71)	IA(0.83)	IA(0.69)	IA(0.70)	IA(0.51)	A(0.61)	IA(0.77)	IA(0.80)	IV
PG_LP48	IA(0.69)	IA(0.83)	IA(0.59)	IA(0.59)	IA(0.57)	IA(0.79)	IA(0.63)	IA(0.74)	IV
PG_LP49	IA(0.69)	IA(0.83)	IA(0.59)	IA(0.59)	IA(0.57)	IA(0.79)	IA(0.63)	IA(0.74)	IV
PG_LP50	IA(0.80)	IA(0.80)	IA(0.59)	IA(0.73)	IA(0.54)	A(0.89)	IA(0.64)	IA(0.71)	IV
PG_LP51	IA(0.80)	IA(0.80)	IA(0.59)	IA(0.73)	IA(0.54)	A(0.89)	IA(0.64)	IA(0.71)	IV
PG_LP52	IA(0.71)	IA(0.87)	IA(0.62)	IA(0.59)	IA(0.58)	A(0.51)	IA(0.61)	IA(0.67)	IV
PG_LP53	IA(0.67)	IA(0.82)	IA(0.59)	IA(0.60)	IA(0.59)	A(0.98)	IA(0.61)	IA(0.75)	IV
PG_LP54	IA(0.68)	IA(0.66)	IA(0.57)	IA(0.76)	IA(0.67)	IA(0.90)	A(0.50)	IA(0.85)	IV
PG_LP55	IA(0.89)	IA(0.91)	A(0.52)	A(0.73)	IA(0.56)	A(0.90)	IA(0.89)	IA(0.97)	V
PG_LP56	IA(0.71)	IA(0.85)	A(0.64)	IA(0.66)	IA(0.70)	IA(0.82)	IA(0.72)	IA(0.78)	IV
PG_LP57	IA(0.71)	IA(0.85)	A(0.64)	IA(0.66)	IA(0.70)	IA(0.82)	IA(0.72)	IA(0.78)	IV
PG_LP58	IA(0.71)	IA(0.83)	IA(0.61)	IA(0.72)	IA(0.52)	A(0.96)	IA(0.67)	IA(0.63)	V
PG_LP59	IA(0.75)	IA(0.79)	IA(0.57)	IA(0.72)	IA(0.56)	IA(0.54)	IA(0.72)	IA(0.78)	IV
PG_LP60	IA(0.78)	IA(0.76)	IA(0.58)	IA(0.68)	IA(0.52)	A(0.91)	IA(0.74)	IA(0.77)	IV
PG_LP61	IA(0.78)	IA(0.77)	IA(0.57)	IA(0.71)	IA(0.51)	A(0.94)	IA(0.66)	IA(0.75)	IV
PG_LP62	IA(0.78)	IA(0.77)	IA(0.57)	IA(0.71)	IA(0.51)	A(0.94)	IA(0.66)	IA(0.75)	IV
PG_LP63	IA(0.62)	IA(0.87)	IA(0.53)	A(0.66)	IA(0.57)	A(0.90)	IA(0.82)	IA(0.86)	IV

PG_LP64	IA(0.75)	IA(0.79)	IA(0.57)	IA(0.72)	IA(0.56)	IA(0.54)	IA(0.72)	IA(0.78)	IV
PG_LP65	IA(0.75)	IA(0.79)	IA(0.57)	IA(0.72)	IA(0.56)	IA(0.54)	IA(0.72)	IA(0.78)	IV
PG_LP66	IA(0.75)	IA(0.79)	IA(0.57)	IA(0.72)	IA(0.56)	IA(0.54)	IA(0.72)	IA(0.78)	IV
PG_LP67	IA(0.70)	IA(0.73)	A(0.60)	IA(0.51)	IA(0.54)	IA(0.93)	IA(0.73)	IA(0.85)	IV
PG_LP68	IA(0.69)	IA(0.82)	IA(0.59)	IA(0.68)	IA(0.63)	A(0.63)	IA(0.74)	IA(0.80)	IV
PG_LP69	IA(0.93)	IA(0.86)	A(0.67)	A(0.87)	IA(0.72)	A(0.90)	IA(0.94)	IA(0.88)	V
PG_LP70	IA(0.69)	IA(0.89)	A(0.62)	IA(0.99)	IA(0.68)	IA(0.87)	A(0.51)	IA(0.99)	III
PG_LP71	IA(0.69)	IA(0.91)	A(0.56)	A(0.55)	IA(0.77)	IA(0.66)	IA(0.58)	IA(0.71)	V
PG_LP72	IA(0.82)	IA(0.88)	A(0.76)	IA(0.67)	IA(0.85)	A(0.66)	IA(0.76)	IA(0.69)	V
PG_LP73	IA(0.80)	IA(0.88)	A(0.75)	IA(0.79)	IA(0.75)	A(0.93)	IA(0.79)	IA(0.69)	V
PG_LP74	IA(0.80)	IA(0.88)	A(0.75)	IA(0.79)	IA(0.75)	A(0.93)	IA(0.79)	IA(0.69)	V
PG_LP75	IA(0.80)	IA(0.89)	A(0.77)	IA(0.96)	IA(0.91)	A(0.98)	IA(0.88)	IA(0.64)	V
PG_LP76	IA(0.58)	IA(0.76)	A(0.66)	IA(0.91)	IA(0.70)	IA(0.97)	IA(0.93)	IA(0.97)	IV
PG_LP77	IA(0.58)	IA(0.76)	A(0.66)	IA(0.91)	IA(0.70)	IA(0.97)	IA(0.93)	IA(0.97)	IV
PG_LP78	A(0.52)	IA(0.74)	IA(0.62)	A(0.71)	A(0.57)	A(0.95)	IA(0.85)	IA(0.99)	IV
PG_LP79	IA(0.82)	IA(0.63)	IA(0.84)	A(0.84)	IA(0.66)	A(0.97)	IA(0.78)	IA(0.98)	V
PG_LP80	IA(0.55)	IA(0.77)	A(0.64)	IA(0.76)	IA(0.54)	IA(0.97)	IA(0.96)	IA(0.93)	IV
PG_LP81	IA(0.65)	IA(0.85)	IA(0.56)	A(0.70)	A(0.63)	A(0.92)	IA(0.87)	IA(0.89)	IV
PG_LP82	IA(0.85)	IA(0.52)	IA(0.93)	IA(0.91)	IA(0.78)	IA(0.98)	IA(0.83)	IA(0.74)	V
PG_LP83	IA(0.85)	IA(0.53)	IA(0.93)	IA(0.91)	IA(0.77)	IA(0.68)	IA(0.88)	IA(0.69)	V
PG_LP84	IA(0.82)	IA(0.59)	IA(0.93)	IA(0.88)	IA(0.76)	IA(0.99)	IA(0.87)	IA(0.79)	V

PG_LP85	IA(0.86)	A(0.51)	IA(0.91)	IA(0.90)	IA(0.60)	IA(0.99)	IA(0.93)	IA(0.75)	V
PG_LP86	IA(0.72)	IA(0.58)	IA(0.89)	IA(0.95)	IA(0.76)	IA(0.99)	IA(0.90)	IA(0.64)	V
PG_LP87	IA(0.81)	A(0.51)	IA(0.92)	IA(0.86)	IA(0.72)	IA(0.94)	IA(0.93)	IA(0.50)	IV
PG_LP88	IA(0.87)	A(0.54)	IA(0.89)	IA(0.85)	IA(0.60)	A(0.99)	IA(0.98)	IA(0.84)	IV
PG_LP89	IA(0.84)	A(0.54)	IA(0.90)	IA(0.75)	IA(0.76)	A(0.55)	IA(0.69)	IA(0.74)	V
SD_1*	A(0.65)	A(0.89)	A(0.70)	IA(0.83)	A(0.50)	IA(0.96)	IA(0.74)	IA(0.90)	VI
SD_2*	IA(0.74)	A(0.89)	IA(0.78)	IA(0.84)	IA(0.69)	IA(0.71)	IA(0.68)	IA(0.67)	IV
SD_3*	IA(0.69)	IA(0.62)	IA(0.74)	IA(0.51)	A(0.52)	A(0.99)	IA(0.51)	IA(0.67)	IV

HT, hepatotoxicity; NeuT, neuro toxicity; NepT, nephrotoxicity; CD, cardiotoxicity; CT, carcinogenicity; IT, immunotoxicity; MT, mutagenicity; CT, cytotoxicity; A, active; IA, inactive.

3.3. Drug-likeness score prediction and frontier molecular orbital analyses

The DL score is another important profile guide to select more potential candidates with a higher chance of clinical success. Based on records, among 89 phytochemicals, 42 showed negative scores as not suitable profiles to be drugs, even showing strong binding affinity. Exclusive analysis taking most of the 7 lead phytochemicals, PG_LP37 and PG_LP22 showed negative DL scores, whereas including PG_LP37, PG_LP81, and PG_LP22 showed poor water solubility (WS), and PG_LP57 and PG_LP56 showed moderate WS profiles. By considering all parameters, PG_LP21 and PG_LP75 are two potential lead phytochemicals (Table 3). From SAR point of view, among the seven, two are the terpenoids class of phytochemicals, and the other five are the phenolic class of phytochemicals, and even though they contain a common moiety, they have shown distinct drug-ability profiles based on functional attachments. For example, if we compare PG_LP21 and PG_LP75, both have nearly similar structures except for an additional glucose moiety in PG_LP75 (Fig. 1), which slightly changes the DL-score and binding efficacy *vice versa* (Table 3; Fig. 3A). As a result, small modifications and attachments vary the potency, toxicity, and drug-ability profile of the candidate, and all parameters are predicted based on individual chemical structure only. In parallel, the analyses of the HOMO, LUMO, and their energy gap (ΔEH-L eV) for the lead phytochemicals PG_LP75 and SD1 were conducted, showing that PG_LP75 has a nearly similar energy gap (10.185 eV) to that of SD1 (10.389 eV), which indicates that PG_LP75 exhibits similar types of reactivity with SD1 against the target (Fig. 3B). Mechanistically, a comparatively large HOMO-LUMO energy gap indicates high kinetic stability and low chemical reactivity (chemical hardness), meaning both PG_LP75 and SD1 are expected to be electronically stable and less prone to undergo unwanted redox reactions or metabolic degradation under physiological conditions; the near-equivalence of their gaps (within 0.2 eV) suggests comparable electronic stability rather than one compound being intrinsically more reactive/unstable than the other, which is a favourable, DL-property for both. Currently, HOMO-LUMO analyse is widely uses in theoretical chemistry to explore the flexibility and rigidity of chemical structures correlated with binding affinity. Overall, drug chemistry and drug-ability prediction guided towards select the lead candidates from library of phytochemicals with higher chance of experimental success.

Table 3: Potency, toxicity, water solubility, pharmacokinetics, and drug-ability profiles of the top fifteen phytochemicals towards election of the most potential lead candidate among them.

Lead candidates	**Average docking**	**Ro5**	**WS**	**BA**	**DL**	**LD50 (mg/kg)**	**Toxicity class**	**GI-abs.**	**BBB permit**

PG_LP37	-8.90	Yes	PS	0.55	-0.22	2000	IV	Low	No
PG_LP75	-8.66	No	S	0.17	0.91	5000	V	Low	No
PG_LP57	-8.86	Yes	MS	0.55	0.16	2000	IV	High	No
PG_LP56	-8.73	Yes	MS	0.55	0.16	2000	IV	High	No
PG_LP81	-8.73	Yes	PS	0.56	0.60	2000	IV	High	No
PG_LP22	-8.43	Yes	PS	0.55	-0.50	1140	IV	Low	No
PG_LP21	-8.36	No	S	0.17	0.93	5000	V	Low	No

BA, bioavailability; DL, drug-likeness; NP, not predicted; Ro5, Lipinski rule of five; SD, standard drugs; WS, water solubility (S, soluble, MS, moderate soluble, PS, poor soluble); BBB, blood brain barrier; LD50, fifty percent lethal dose.

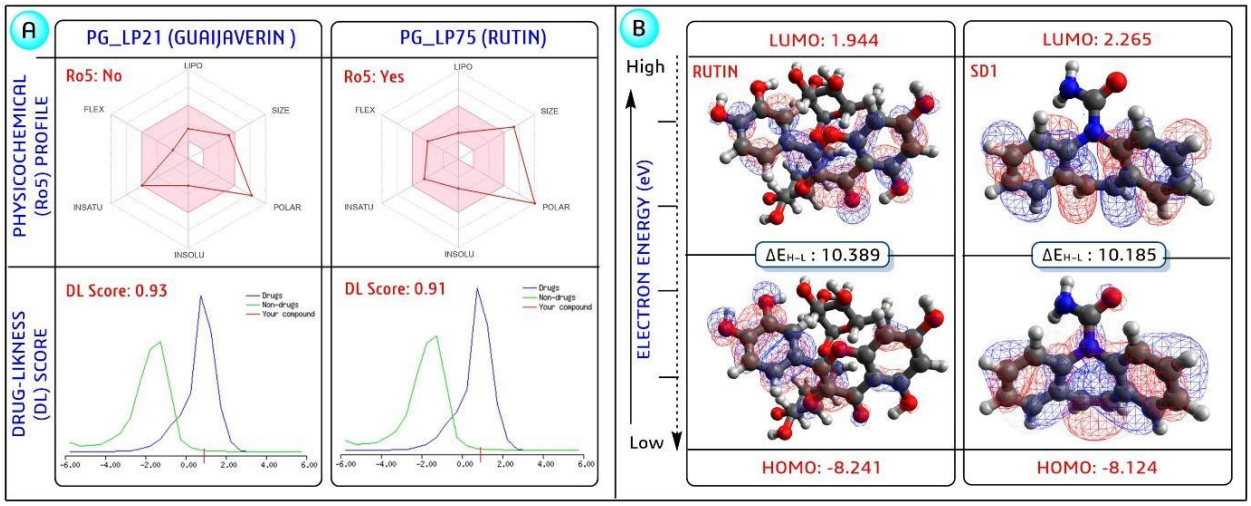

Figure 3: (**A**), Graphic presentation of physicochemical properties (Ro5), and drug-likeness (DL) score of two lead phytochemicals (PG_LP21 and PG_LP75), and (**B**), the HOMO-LUMO energy plot of the most lead phytochemical (PG_LP75) and SD1 (carbamazepine). The ChemDraw 2020 software was used to visualize the picture.

3.4. Molecular dynamics simulation and free-energy calculation

The selected lead phytochemical (PG_LP75/rutin) and standard drug (SD_1/Carbamazepine) with SCN1A MD simulation results at 100 ns were recorded in Fig. 4. The molecular stability and kinetic behaviours were observed based on plotted RMSD, RMSF, Rg, and the number of H-bond interaction plots (Figs. 4A-4F). The backbone protein RMSD plots (Fig. 4A) and ligand RMSD (Fig. 4B) indicated protein RMSD showed nearly similar deviation, but ligand RMSD clearly indicated that PG_LP75 had higher stability than SD1. Specifically, the near-identical protein backbone RMSD in both complexes indicates that neither ligand caused any large-scale conformational perturbation of the SCN1A fold, while the comparatively lower and steadier ligand RMSD for PG_LP75 suggests that rutin remained more consistently anchored within its binding pocket than carbamazepine, which showed relatively larger positional fluctuation, consistent with weaker positional restraint at the docking site. Although RMSF and Rg plots looking similar types, but when observed minutely PG_LP75 had higher stability than SD1 with SCN1A (Figs. C and D). The SCN1A- PG_LP75 maximum five and 3 as constant through the simulation time (Fig. 4E), where SCN1A-SD1 complex displayed only one H-bond throughout 100 ns (Fig. 4F), clearly indicated that due to higher number of H-bonds interactions, PG_LP75 showed higher docking score as well stability than SD1. The RMSF profile (Fig. 4C) was elevated mainly at flexible loop/terminal segments of SCN1A in both complexes, while residues lining the docking pocket showed comparatively restrained fluctuation, and the radius of gyration (Fig. 4D) remained essentially

constant throughout the 100 ns run for both systems, together indicating that the overall protein fold was structurally maintained and that the differences observed were localized to the ligand-binding region rather than reflecting global protein destabilization. The sustained multi-point hydrogen bonding of PG_LP75 (up to five bonds, Fig. 4E) versus the single, intermittent hydrogen bond of carbamazepine (Fig. 4F) is consistent with rutin's larger number of hydroxyl/glycosidic hydrogen-bond donor-acceptor groups, offering a plausible structural explanation for its comparatively higher positional stability in this static docking/MD framework. Additionally, the free energy calculation method (MM/PBSA) showed that the SCN1A-PG_LP75/rutin complex had a free energy of -66.79 kcal/mol., while the SCN1A-SD_1/Carbamazepine complex had -45.38 kcal/mol., indicating that PG_LP75/rutin had the lower energy, representing a stronger binding affinity than SD1, as exhibited in the docking score (Figs. 5A and 5C). Nonetheless, both chemicals belong to different chemical classes and interact with the same SCN1A at different residues (Figs. 5B and 5D). Overall, PG_LP75/rutin demonstrated higher stability and free energy to be an ideal lead candidate for further experimental validation.

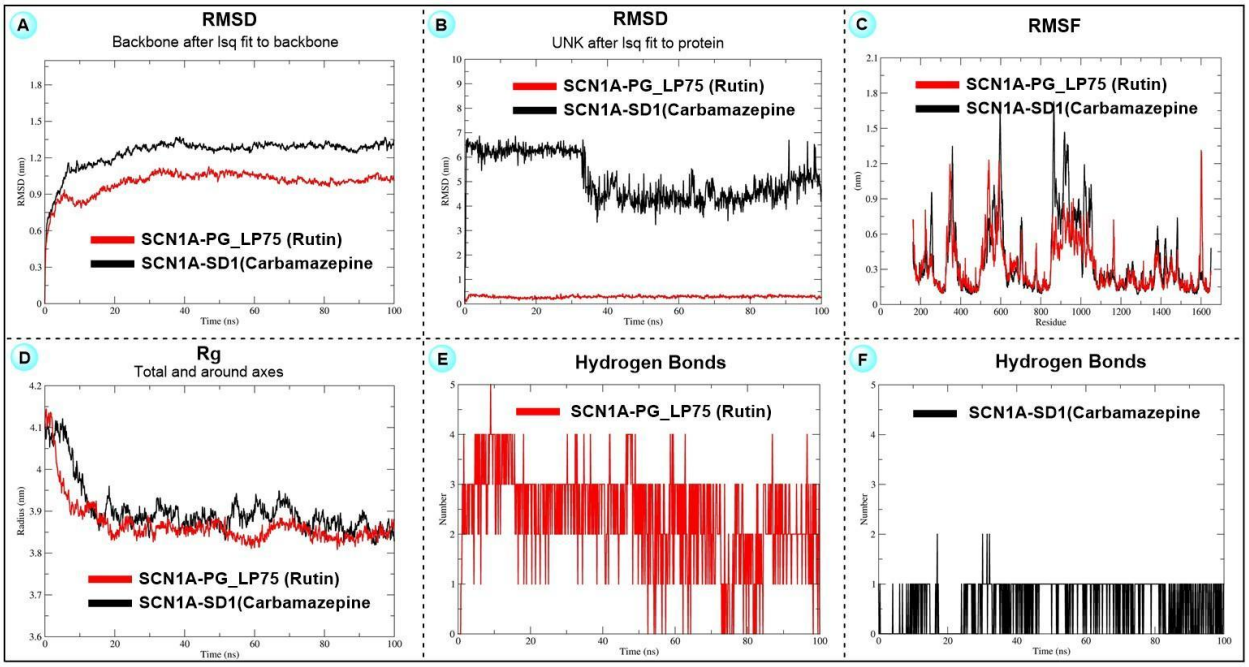

Figure 4: The analysis of conformational stability includes RMSD, RMSF, and Rg-score plots for the docking complexes of SCN1A-PG_LP75 (rutin) and SCN1A-SD1 (carbamazepine) over a period of 100 nanoseconds. The following plots are presented: (**A**) RMSD plots of the backbone protein; (**B**) RMSD plots of the ligand; (**C**) RMSF plots; (**D**) Rg plots; (**E**) H-bond interaction plot for SCN1A-PG_LP75; and (**F**) H-bond interaction plot for SCN1A-SD1.

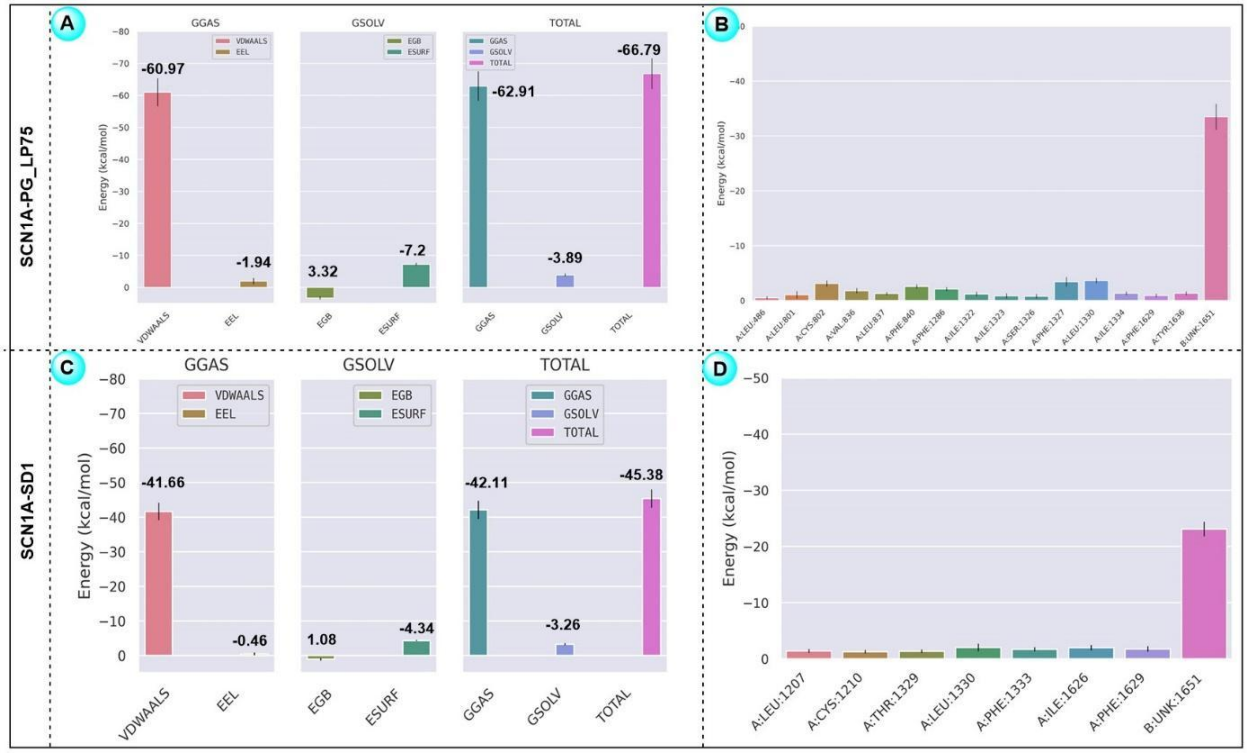

Figure 5: The free energy (ΔGbind) calculation using the MM/PBSA method; A and B present the energy components of PG_LP75, and C and D for the SD1 docking complex with SCN1A.

4. Discussion

The present study utilized an integrated computational approach to assess the therapeutic potential of phytochemicals derived from *P. guajava* leaves, aiming to substantiate traditional medicinal claims to lead identification for HE. Although crude extracts exhibited potential activity, variability and lack of mechanistic clarity limited their mainstream application, whereas the target-specific strategy provides precision, reproducibility, and selective efficacy. The selected lead (rutin) is also supported by existing literature as effective for chronic liver disorder and neuroprotective (44-47). As at an individual level rutin showed hepatoprotective, anti-inflammatory, and neuroprotective potency, it is expected to be effective against HE. On the other hand, phytochemicals struggling for FDA approval face especially significant challenges for low solubility and poor pharmacokinetics, as most phytochemicals do not succeed in clinical trial phases (48-50). In this perspective, to limit the hit-and-trial investigation and random expensive experimental studies, advanced bioinformatics and chemoinformatics tools help to accelerate and guide lead drug selection with a higher chance of clinical success. Currently, researchers widely use computational studies like docking simulation to streamline selection within limited resources and increase the likelihood of high experimental success. Overall, target-specific drug discovery with other drug-ability parameter predictions helps to bridge the gap between traditional medicine and modern pharmacology, providing opportunities for their integration into mainstream therapeutics with greater scientific rigor (36, 37).

From a mechanistic standpoint, it is worth noting that the three selected targets act through distinct pharmacological mechanisms: SCN1A is a state-dependent ion channel typically inhibited via a conformation-specific pore-blocking mechanism, GLDC is a pyridoxal-5'-phosphate-dependent metabolic enzyme whose inhibition would reduce glycine cleavage and, consequently, ammonia/glycine-related neurotoxicity, and KCNQ2 is a voltage-gated potassium channel whose opening (rather than blockade) is anticonvulsant. Because rutin (PG_LP75) is a polyphenolic flavonol glycoside with well-documented antioxidant and membrane-interacting properties, its predicted activity across these mechanistically distinct targets is biologically plausible primarily as a multi-target modulator

acting through hydrogen-bonding/aromatic-stacking interactions at each binding pocket, rather than through a single unifying catalytic mechanism; this multi-target profile is consistent with existing pharmacological reports describing rutin's hepatoprotective, anti-inflammatory, antioxidant, and neuroprotective activities across diverse molecular targets (44-47). Comparable target-specific CADD screening pipelines applied to other medicinal plants have reported similar docking score ranges (-4 to -12 kcal/mol.) and a similarly low overall hit rate (a small minority of the screened library qualifying as leads after combined potency, Ro5, and toxicity filtering), supporting the generalizability of the present multi-parameter screening funnel (36, 38, 43). Nonetheless, because HE is a multifactorial neurometabolic syndrome and the present evidence is derived entirely from static structure-based methods, these findings should be interpreted as hypothesis-generating rather than confirmatory of clinical efficacy.

Simultaneously, a proper hypothesis and background knowledge on bioinformatics tools play the most effective role in getting the reliable results. Because most tools and software are run through a set of algorithms and programming languages, there is a high chance of error generation, where certain expertise helps to select ideal tools as well as minimize the error. Computational studies do not provide the concentration or dose needed for therapeutic value; therefore, rigorous cross-verification in experimental studies is necessary, as recommendations cannot be made based solely on computational data. Overall, the computational platforms have revolutionized the drug discovery module by selecting lead products in a comprehensive framework (36, 43). This is especially valuable in evaluating phytochemicals from medicinal plants, where complex mixtures and limited experimental data pose challenges to traditional pharmacological approaches. A limitation of the present study is that the 100 ns MD simulation and MM/PBSA free-energy analysis were performed only for the SCN1A-PG_LP75 and SCN1A-SD1 complexes; the strong docking interactions predicted for PG_LP75 (and other lead phytochemicals) against GLDC and KCNQ2 were not dynamically validated here and represent a priority for follow-up work. We encourage independent replication and extension of this workflow to the remaining targets as a next step toward experimental validation. At present, due to lack of a robust facility, we are unable to incorporate such things but will try it in the future through collaboration.

5. Conclusion

This study provides a comprehensive computational-based investigation into the target-specific therapeutic efficacy of *P. guajava* leaf-derived phytochemicals against HE. Leveraging traditional knowledge of *P. guajava* as a hepatoprotective and neuroprotective agent, we systematically screened 89 bioactive phytochemicals extracted from various solvent systems. Through a target-driven *in silico* strategy, four key HE-associated molecular targets, SCN1A, GLDC, and KCNQ2, were selected based on their relevance in HE pathophysiology and retrieved from the GeneCards database. Molecular docking studies revealed several phytochemicals showed strong binding affinities compared to standard drugs. Further, all drug-able parameters for each phytochemical were predicted and analysed, with PG_LP21 (guaijaverin) and PG_LP75 (rutin) selected as lead candidates. Additional MD simulations and free energy calculations confirmed stable protein–ligand interactions, while HOMO–LUMO analysis validated the electronic viability and reactivity of the lead phytoconstituent, surpassing that of the standard drug. Overall, this study provides a solid starting point for looking into *P. guajava* as a source of plant-based treatments for HE, and future work should focus on testing the promising compounds found, as well as creating formulations that enhance their absorption and effectiveness in special cases.

6. Acknowledgements

This work is a part of the Ph.D. thesis work of Mr. Debasis Patra, Centurion University of Technology and Management, Odisha. The authors gratefully acknowledge the Honorable Vice-Chancellor of Centurion University for permitting Ph.D. registration, continuous encouragement, and providing essential facilities and institutional support. The authors also sincerely thank the Director of Salixiras Research Private Limited, Bhubaneswar, for extending access to advanced computational infrastructure that was instrumental in completing this research work.

Declaration of competing Interest

The authors declare that they have no competing of interests.

Data Availability

Data will be made available on request.

REFERENCES

1. Wijdicks EF. Hepatic Encephalopathy. N Engl J Med. 2016; 375(17):1660-1670.
2. Krishnarao A, Gordon FD. Prognosis of Hepatic Encephalopathy. Clin Liver Dis. 2020; 24(2):219-229.
3. Rudler M, Weiss N, Bouzbib C, Thabut D. Diagnosis and Management of Hepatic Encephalopathy. Clin Liver Dis. 2021; 25(2):393-417.
4. Rose CF, Amodio P, Bajaj JS, Dhiman RK, Montagnese S, Taylor-Robinson SD, Vilstrup H, Jalan R. Hepatic encephalopathy: Novel insights into classification, pathophysiology and therapy. J Hepatol. 2020; 73(6):1526-1547.
5. Elsaid MI, Rustgi VK. Epidemiology of Hepatic Encephalopathy. Clin Liver Dis. 2020; 24(2):157-174.
6. Juanola A, Pose E, Ginès P. Liver Cirrhosis: ancient disease, new challenge. Med Clin (Barc). 2025; 164(5):238-246.
7. Duah A, Agyei-Nkansah A, Osei-Poku F, Duah F, Ampofo-Boobi D, Peprah B. The Prevalence, Predictors, and In-Hospital Mortality of Hepatic Encephalopathy in Patients with Liver Cirrhosis Admitted at St. Dominic Hospital in Akwatia, Ghana. Can J Gastroenterol Hepatol. 2020; 2020:8816522.
8. Karki U, Upreti N, Gyawali B, Shrestha SK, Basnet CK, Sharma D, Dangol N. Hepatic Encephalopathy among Patients with Chronic Liver Disease Admitted to the Department of Internal Medicine in a Tertiary Care Centre: A Descriptive Cross-sectional Study. JNMA J Nepal Med Assoc. 2023; 61(263): 580-583.
9. Sepehrinezhad A, Shahbazi A. Linking Brain and Immune Transcriptomes to Gut-Derived Metabolites in Hepatic Encephalopathy: An Explorative Integrative Multi-Omics Approach. Hepat Med. 2025; 17:105-124.
10. Gan C, Yuan Y, Shen H, Gao J, Kong X, Che Z, Guo Y, Wang H, Dong E, Xiao J. Liver diseases: epidemiology, causes, trends and predictions. Signal Transduct Target Ther. 2025; 10(1):33.
11. Luo X, He Y, Jiang Z, Liao J. Global burden of liver cirrhosis: trends from 1990-2021 and projections to 2060. J Health Popul Nutr. 2025; 44(1):370.
12. Louissaint J, Deutsch-Link S, Tapper EB. Changing Epidemiology of Cirrhosis and Hepatic Encephalopathy. Clin Gastroenterol Hepatol. 2022; 20(8S): S1-S8.
13. Indian Society of Gastroenterology (ISG). Indian Journal of Gastroenterology. 2018; 37: 1-137.
14. Vishnupriya, Chinnam; Sreekrishnan, T. P.; Gireesh Kumar, K. P.; Dhanasekaran, B. S.; Hrushikesh, Anagani. Clinical Profile and Outcomes of Hepatic Encephalopathy in Cirrhotic Patients Admitted to the Emergency Department in Kerala, India. Amrita Journal of Medicine 2025; 21(3): 141-146.
15. Kimer N, Krag A, Gluud LL. Safety, efficacy, and patient acceptability of rifaximin for hepatic encephalopathy. Patient Prefer Adherence. 2014; 8:331-8.
16. Sharma P, Sharma BC. Management of overt hepatic encephalopathy. J Clin Exp Hepatol. 2015; 5(1): S82-7.
17. Wang Z, Chu P, Wang W. Combination of rifaximin and lactulose improves clinical efficacy and mortality in patients with hepatic encephalopathy. Drug Des Devel Ther. 2018; 13:1-11.
18. European Association for the Study of the Liver. EASL Clinical Practice Guidelines on the management of hepatic encephalopathy. J Hepatol. 2023; 79(5):1340.
19. Higuera-de-la-Tijera F, Alvares-da-Silva MR, Castro-Narro GE, Barahona-Garrido J, Carrera-Estupiñán E, Garavito-Rentería J, Henríquez-Meléndez HA, Hernández-Cely G, Mora-Lazo J, Mendizabal M, Mezzano-Puentes GA, Oliveira CP, Guimarães Pessoa M, Suárez-Quintero Y, Velarde-Ruiz Velasco JA. First Latin American consensus on the treatment and prophylaxis of hepatic encephalopathy. Ann Hepatol. 2025; 31(1):102142.
20. Philips CA, Augustine P, Rajesh S, Y PK, Madhu D. Complementary and Alternative Medicine-related Drug-induced Liver Injury in Asia. J Clin Transl Hepatol. 2019; 7(3):263-274.
21. Gittinger FS, Rahnfeld A, Lacruz E, Zipprich A, Lammert F, Ripoll C. Use of complementary and alternative medicine in patients with chronic liver diseases in Germany- a multicentric observational study. BMC Complement Med Ther. 2024; 24(1):340.
22. Gillessen A, Schmidt HH. Silymarin as Supportive Treatment in Liver Diseases: A Narrative Review. Adv Ther. 2020; 37(4):1279-1301. doi: 10.1007/s12325-020-01251-y.
23. Frozandeh F, Shahrokhi N, Khaksari M, Amiresmaili S, AsadiKaram G, Shahrokhi N, Iranpour M. Evaluation of the protective effect of curcumin on encephalopathy caused by intrahepatic and extrahepatic damage in male rats. Iran J Basic Med Sci. 2021; 24(6):760-766.
24. Das R, Mitra S, Tareq AM, Emran TB, Hossain MJ, Alqahtani AM, Alghazwani Y, Dhama K, Simal-Gandara J. Medicinal plants used against hepatic disorders in Bangladesh: A comprehensive review. J Ethnopharmacol. 2022; 282:114588.
25. Islam Shawon S, Nargis Reyda R, Qais N. Medicinal herbs and their metabolites with biological potential to protect and combat liver toxicity and its disorders: A review. Heliyon. 2024; 10(3): e25340.
26. Zakaria Z, Othman ZA, Nna VU, Mohamed M. The promising roles of medicinal plants and bioactive compounds on hepatic lipid metabolism in the treatment of non-alcoholic fatty liver disease in animal models: molecular targets. Arch Physiol Biochem. 2023; 129(6):1262-1278.

27. Thilagavathi R, Begum SS, Varatharaj SD, Balasubramaniam AK, George JS, Selvam C. Recent insights into the hepatoprotective potential of medicinal plants and plant-derived compounds. Phytotherapy Research. 2023; 37(5):2102-18.
28. Ali SA, Datusalia AK. Protective effects of Tinospora cordifolia miers extract against hepatic and neurobehavioral deficits in thioacetamide-induced hepatic encephalopathy in rats via modulating hyperammonemia and glial cell activation. J Ethnopharmacol. 2024; 323:117700.
29. Gutiérrez RM, Mitchell S, Solis RV. *Psidium guajava*: a review of its traditional uses, phytochemistry and pharmacology. J Ethnopharmacol. 2008;117(1):1-27.
30. Díaz-de-Cerio E, Verardo V, Gómez-Caravaca AM, Fernández-Gutiérrez A, Segura-Carretero A. Health Effects of *Psidium guajava* L. Leaves: An Overview of the Last Decade. Int J Mol Sci. 2017; 18(4):897.
31. Chechani B, Roat P, Hada S, Yadav DK, Kumari N. *Psidium guajava*: An Insight into Ethnomedicinal Uses, Phytochemistry, and Pharmacology. Comb Chem High Throughput Screen. 2024; 27(1):2-39.
32. Butt E, Altemimi AB, Younas A, Butt MS, Jalal M, Bhatty M, Abdi G, Aadil RM. Guava (*Psidium guajava*): A brief overview of its therapeutic and health potential. Food Chem X. 2025; 31:103027.
33. Liu C, Jullian V, Chassagne F. Ethnobotany, phytochemistry, and biological activities of *Psidium guajava* in the treatment of diarrhea: a review. Front Pharmacol. 2024; 15:1459066.
34. Gouri V, Upreti S, Samant M. Evaluation of target-specific natural compounds for drug discovery against Leishmaniasis. Parasitol Int. 2022; 91:102622.
35. Li J, Beaudoin C, Ghosh S. Energy-based generative models for target-specific drug discovery. Front Mol Med. 2023; 3:1160877.
36. Swain SS, Hussain T. Combined Bioinformatics and Combinatorial Chemistry Tools to Locate Drug-Able Anti-TB Phytochemicals: A Cost-Effective Platform for Natural Product-Based Drug Discovery. Chem Biodivers. 2022; 19(11): e202200267.
37. Talevi A. Computer-Aided Drug Discovery and Design: Recent Advances and Future Prospects. Methods Mol Biol. 2024; 2714:1-20.
38. Sahoo A, Swain SS, Pakeeraiah K, Paidesetty SK, Panda M. Design, synthesis of next generation indomethacin-based cyclooxygenase-2 inhibitor: An *in silico* and *in vitro* investigation. Int J Biol Macromol. 2025; 331(1):148263.
39. Khraim W, Abu-Libdeh B, Ayesh S, Dweikat I. Clinical heterogeneity of glycine encephalopathy in three Palestinian siblings: A novel mutation in the glycine decarboxylase (GLDC) gene. Brain Dev. 2017; 39(7):601-605.
40. Lu X, Li K, Yang J. Potassium voltage-gated channel subfamily D member 2 induces an aggressive phenotype in lung adenocarcinoma. Neoplasma. 2021; 68(1):135-143.
41. Li N, Yan L, Peng A, Fu X, Qin H, Yao K. Voltage-gated sodium channels in the nervous system: Molecular physiology to therapeutic interventions. Neural Regen Res. 2025. doi: 10.4103/NRR.NRR-D-25-00260.
42. Swain SS, Sahoo A, Singh SR, Sahoo J, Paidesetty SK. Synthesis, spectroscopic analysis, and computational-based investigations on 'azo-coumarin-Co(II)-galangin' hybrids exhibit multipotential activities. J Biomol Struct Dyn. 2025; 43(14):7336-7347.
43. Sahoo A, Swain SS, Singh SR, Jena AB, Paidesetty SK, Duttaroy AK, Panda M. Target-specific therapeutic assessment of repurposed drug candidates for oral lichen planus: a network pharmacology-molecular dynamics simulation guided investigation. BDJ Open. 2025 11(1):99.
44. Swain SS, Sahoo SK. Piperlongumine and its derivatives against cancer: A recent update and future prospective. Arch Pharm (Weinheim). 2024; 357(7): e2300768.
45. Rahmani S, Naraki K, Roohbakhsh A, Hayes AW, Karimi G. The protective effects of rutin on the liver, kidneys, and heart by counteracting organ toxicity caused by synthetic and natural compounds. Food Sci Nutr. 2022; 11(1):39-56.
46. Anwar MM, Laila IMI. The ameliorating effect of Rutin on hepatotoxicity and inflammation induced by the daily administration of vortioxetine in rats. BMC Complement Med Ther. 2024; 24(1):153.
47. Chunmei Z, Shuai W. Molecular mechanisms of neuroprotective effect of rutin. Front Pharmacol. 2025; 16:1599167.
48. Feng Y, Peng L, Liu X, Zheng Q, Qian M, Deng M, Peng J, Li Y, Lin L, Peng Q. Rutin-Associated Hepatoprotection: A Review of Mechanisms and Therapeutic Prospects. Basic Clin Pharmacol Toxicol. 2025; 136(6): e70042.
49. Wang Z, Sun X, Sun M, Wang C, Yang L. Game Changers: Blockbuster Small-Molecule Drugs Approved by the FDA in 2024. Pharmaceuticals (Basel). 2025; 18(5):729.
50. Rajpoot S, Kumar R, Singh R, Chandel S. Advancements in neuroblastoma treatment: FDA-approved drugs and role of phytochemicals. Mol Biol Rep. 2025; 52(1):516.